FOSSIL ENERGY

DOE/BC/15211-6
(OSTI ID: 756596)

THE DYNAMICS OF COMBUSTION FRONTS IN POROUS MEDIA

Topical Report
June 2000

By
İ. Yücel Akkutula
Yannis C. Yortsos

Date Published: June 2000

Work Performed Under Contract No. DE-AC26-99BC15211

University of Southern California
Los Angeles, California

National Petroleum Technology Office
U.S. DEPARTMENT OF ENERGY
Tulsa, Oklahoma

DOE/BC/15211-6
Distribution Category UC-122

The Dynamics of Combustion Fronts in Porous Media

By
İ. Yücel Akkutula
Yannis C. Yortsos

June 2000

Work Performed Under Contract No DE-AC26-99BC15211

Prepared for
U.S. Department of Energy
Assistant Secretary for Fossil Energy

Thomas B. Reid, Project Manager
National Petroleum Technology Office
P.O. Box 3628
Tulsa, OK 74101

Prepared by
Department of Chemical Engineering
University of Southern California
University Park Campus – HEDCO 316, USC
Los Angeles, CA 90089-1211

Table of Contents

Abstract

The sustained propagation of combustion fronts in porous media is a necessary condition for the success of an in-situ combustion project for oil recovery. Compared to other recovery methods, in-situ combustion involves the added complexity of exothermic chemical reactions and temperature-dependent chemical kinetics. This gives rise to reaction zones of a spatially narrow width, within which heat release rates, temperatures and species concentrations vary significantly. This sharp variation makes difficult the simulation of combustion processes using coarse grids and the implementation of upscaling methods.

In this paper, we propose a method for solving this problem by treating the reaction region as a place of discontinuities in the appropriate variables, which include, for example, fluxes of heat and mass. Using a rigorous perturbation approach, similar to that used in the propagation of flames [3], and smoldering combustion [7], we derive appropriate jump conditions that relate the change in these variables across the front. These conditions account for the kinetics of the reaction between the oxidant and the fuel, the changes in the morphology of the pore space and the heat and mass transfer in the reaction zone. Then, the modeling of the problem reduces to the modeling of the dynamics of a combustion front, on the regions of either side of which transport of momentum (fluids), heat and mass, but not chemical reactions, must be considered. Properties of the two regions are coupled using the derived jump conditions. This methodology allows to explicitly incorporate permeability heterogeneity effects in the process description, without the undue complexity of the coupled chemical reactions.

1 Introduction

The propagation of combustion fronts in porous media is a subject of interest to a variety of applications, ranging from the in-situ combustion for the recovery of oil [1], to filtration combustion [5] and to smoldering combustion [7]. While these problems may differ in application and context, they share a common characteristic, namely that the main combustion reaction involves the burning of a stationary solid fuel, which in the first two applications is part of the initial state of the system, while in the second it is created by a preceding Low-Temperature-Oxidation (LTO) process. In-situ combustion for oil recovery has been studied quite extensively since the mid 1950s. The two texts by Prats [1] and Boberg [2] summarize the relevant literature on the subject until the late 1980s. A large number of experimental, analytical and numerical studies have been reported on a variety of in-situ combustion topics.

Of interest to this paper is a particular but important issue of in-situ combustion, specifically the dynamics of combustion fronts. They are influenced by a number of factors, including fluid flow of injection and produced gases, mass transfer of the injected oxidant, heat transfer in the porous medium and the surroundings, the rate of reaction(s), the heterogeneity of the medium and possibly the evolution of the pore morphology due to the combustion reaction. Understanding the dynamics is important to a number of issues, including front stability, the sustained propagation of combustion, the effects of heterogeneity, and the scale-up of the process. A specific feature that distinguishes combustion fronts from other front propagation problems is that due to the strong temperature dependence of the reaction rate, the combustion reaction occurs within a thin reaction zone, the extent of which is quite small, and certainly much smaller than the typical grid in field simulation. As a result, it is almost imperative to treat the reaction zone as a surface of discontinuity (a thin layer) within which the combustion reaction occurs, and across which appropriate conditions must apply. The propagation of frontal discontinuities makes the scale-up

of the process a problem qualitatively different than ordinary displacement processes in porous media, for instance waterflooding.

The treatment of combustion fronts as frontal discontinuities has been studied extensively in the literature of combustion and flames. Among the great deal of articles published in this field we will refer to the earlier work of Matalon and Matkowsky [3], the monograph of Pelcé [4] and the more recent work of Schult and co-workers [7]. Ref. [3] discussed the propagation of flames in the combustion of premixed gases, in the absence of a porous medium, and treated the flame front as a surface of discontinuity, which separates two regions of different temperature and chemical composition. To capture phenomena occuring within the thin flame region, the methods of singular perturbation and matched asymptotic expansions were used. Pelcé [4] presents an interesting compilation of studies on combustion and flame propagation in a variety of geometries. In his work, common aspects are shown to exist between the seemingly different problems of viscous displacements in a Hele-Shaw cell (which gives rise to viscous fingering), dendritic solidification and flame propagation. This connection, and particularly with the viscous fingering problem, is of particular interest to our problem of combustion in porous media, as they are both subject to the effects of the medium heterogeneity and other factors. More recently, Aldushin and Matkowsky [5] have used this analogy to argue about the problem of the selection of the width of the Saffman-Taylor finger. We note in passing that the growth of a new phase in a porous medium, driven by diffusion, for example bubble growth in solution gas-drive processes, also shows common aspects with viscous displacements e.g. see Li and Yortsos [6].

In a recent series of papers, Schult et al. [7], [8] studied the combustion of a solid fuel embedded in a homogeneous porous medium. This problem, known as smoldering or filtration combustion, appears in a variety of applications. It differs in many respects from in-situ combustion, particularly on the lack of

liquid flow ahead of the combustion front and the various physicochemical changes that accompany it, the fact that the solid fuel is a priori available, rather than being generated as a result of LTO, as is the case with in-situ combustion, and the existence of heterogeneities. At the same time, the two problems have the common feature of the propagation of a high-temperature reaction zone in which a gas-solid reaction process takes place. Schult et al. [7], [8] provided an asymptotic analysis of the problem following an approach essentially similar to the flame analysis of Ref. [3]. An analogous approach was attempted earlier by Britten and Krantz [14],[15] who examined the structure of the reaction zone in reverse combustion in the context of gasification.

In this paper, we will proceed to analyze the problem of in-situ combustion, by working along very similar lines. We must note that few related theoretical studies exist in the literature of in-situ combustion. Gottfried [9] modeled in-situ combustion by focusing on heat transfer and representing the combustion front as a discontinuity involving a point heat source, represented as a delta function. Beckers and Harmsen [10] detailed the propagation of various regimes in in-situ combustion and its variants (such as wet combustion). Burger and Sahuquet [11] analyzed the chemical aspects of the reaction processes. Ağca and Yortsos [12] proposed a simplified description, which takes into account the heat losses to the surroundings and discussed issues of sustained propagation and extinction. The stability of combustion fronts was analyzed by Armento and Miller [13] using a simplified front analysis.

The paper is organized as follows: First, we provide a simplified approach using the method of characteristics, to define the large-scale features of the temperature profile and delineate the main heat transfer regimes in in-situ combustion. Then, we present the framework of the analysis and proceed with a detailed asymptotic treatment of the reaction front. The jump conditions derived are subsequently used to analyze the properties of planar combustion fronts. Finally, we comment on effects of heterogeneity and

scale-up. Our model is a continuum model, in which effective values are used for the kinetic and transport parameters. A parallel effort is curently being conducted to model combustion at the pore-network scale (Lu and Yortsos, [16]), in order to understand the process at the small scale and to explain the formation of patterns in recent combustion experiments in Hele-Shaw cells [17].

1.1 Large-Scale Features of the Temperature Profile

Before we proceed, we consider a simplified analysis to derive some large-scale features of the typical temperature profile expected in in-situ combustion. For this, we formulate the energy balance in 1-D, when heat conduction is considered negligible compared to convection and consider the solution of a simple case in which the heat of reaction is a Dirac delta function. A justification of this assumption will appear later in this paper. Assuming a constant flow velocity $\tilde{v}$ and neglecting heat conduction we have

$$[(1-\phi)c_s\rho_s]\frac{\partial \tilde{T}}{\partial \tilde{t}} + c_g\rho_g\tilde{v}\frac{\partial \tilde{T}}{\partial \tilde{x}} = \tilde{Q}\delta\left(\tilde{x}-\tilde{x}_f(\tilde{t})\right) - h(\tilde{T}-\tilde{T}_o) \tag{1}$$

where the right-hand side involves the heat of reaction, due to combustion, and a convective-type expression for heat losses to the surroundings. In this notation, $\tilde{Q}$ expresses heat released per unit area and unit time. Initial conditions involve constant temperature $\tilde{T}_o$, initially and at injection ($\tilde{x}=0$).

Consider, first, the case where heat losses are negligible. Equation (1) is a hyperbolic equation with a singular source term at the combustion front $\tilde{x}=\tilde{x}_f(t)$. Outside of the front, the source term is negligible, and the solution of (1) is given using the method of characteristics, which in the present case are straight lines with a constant slope

$$\frac{d\tilde{x}}{d\tilde{t}} = \frac{c_g\rho_g\tilde{v}}{(1-\phi)c_s\rho_s} \equiv U. \tag{2}$$

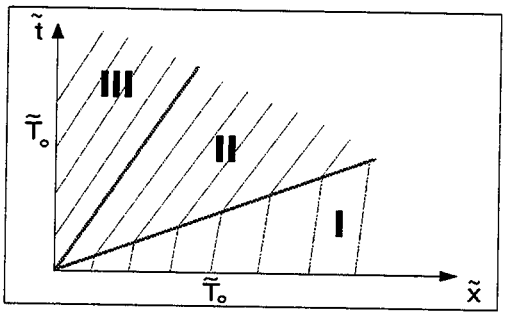

Figure 1: Characteristics Diagram for Combustion

Along the characteristics the temperature is constant. In general, there would be two characteristic velocities, one upstream (denoted by subscript III) and one downstream (denoted by subscript I) of the front, as the consumption and/or production of gases at the reaction front will affect the mass flux. Let the combustion front move with constant velocity V. If conditions are such that

$$V > U_I \quad \text{and} \quad V > U_{III} \tag{3}$$

the characteristics from the initial condition (the $\tilde{x}$-axis) will intersect the front trajectory (Figure 1), while those from the boundary (the $\tilde{t}$-axis) will not, creating an expanding simple wave region (region II in Fig. 1). In this case, the $(\tilde{t} - \tilde{x})$ plane consists of three regions, one corresponding to the initial (region I, of temperature $\tilde{T}_o$), another corresponding to the simple wave (region II, of a temperature to be determined), and a third corresponding to the injection (region III, of temperature $\tilde{T}_o$). The temperature across the front jumps to the value $\tilde{T}_f$, obtained by integrating the energy equation (1) across the combustion front,

$$\tilde{T}_f - \tilde{T}_o = \frac{\tilde{Q}}{[(1-\phi)c_s\rho_s](V - U_I)} \tag{4}$$

A more rigorous expression will be obtained later. Under condition (3), the simple wave region is also spanned by characteristics of slope U_{III}, except that these now emanate from the combustion front (as

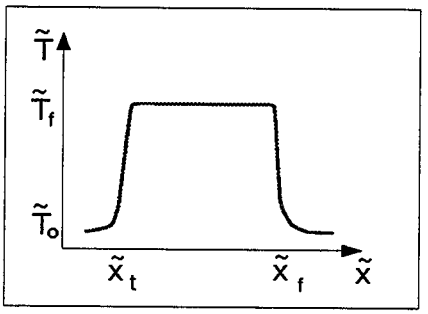

Figure 2: Temperature Profile for the Adiabatic Case

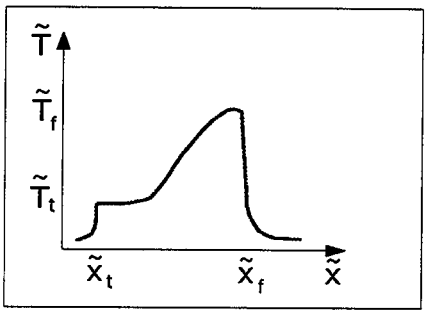

Figure 3: Temperature Profile for Adiabatic Sytem

shown in Figure 1), hence they carry temperature $\tilde{T}_f$. Thus, the temperature profile at any time consists of two far-field regions with temperature $\tilde{T}_o$ and an intermediate expanding region of temperature $\tilde{T}_f$. This profile is sketched in Figure 2. Accounting for conduction will smoothen the discontinuities at the fronts. In realistic cases, heat losses cannot be neglected. If we take the simple linear heat loss term shown in (1), the temperature in region II is not constant any longer, but decreases with time. We can readily show that the solution in this region is

$$\tilde{T} = \tilde{T}_o + (\tilde{T}_f - \tilde{T}_o)\exp\left[-\frac{h(V\tilde{t} - \tilde{x})}{[(1-\phi)c_s\rho_s](V - U_{III})}\right] \tag{5}$$

suggesting an exponential decay. The resulting profile is sketched schematically in Figure 3. Note that the temperature at the trailing edge of the region, $\tilde{T}_t$, declines exponentially in time as

$$\tilde{T}_t = \tilde{T}_o + (\tilde{T}_f - \tilde{T}_o)\exp\left[-\frac{h\tilde{t}}{(1-\phi)c_s\rho_s}\right] \tag{6}$$

The situation is reversed, if the two inequalities (3) are reversed. Now the front moves slower, and it is the temperature downstream, which increases to $\tilde{T}_f$. Region II precedes, rather than trailing the combustion front, the simple wave expanding ahead of it. Analogous conclusions can be reached if one only of the inequalities in (3) is valid, etc.

Having obtained a qualitative understanding of the problem, we will now proceed with a more rigorous analysis.

2 Formulation of the Problem

Typically, combustion reactions have large activation energies. A dimensionless measure is the Zeldovich number, $Z = \frac{E\tilde{T}_o}{R\tilde{T}_f^2}$, where E is the activation energy and $\tilde{T}_f$ denotes the front temperature (a simple expression for which was given in (4)). Typically, Z is large. Because of this condition and the fact

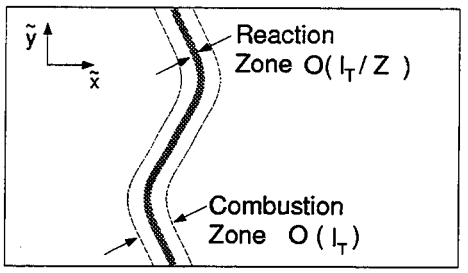

Figure 4: Definition of Reaction and Combustion Zones

that the reaction rate is strongly temperature dependent, all combustion reactions are confined to a thin reaction-dominated zone at the combustion front. It is within this m zone, where reactions occur at a high rate, temperature, pressure and concentrations being approximately constant. The reaction zone is embedded within the heat transfer layer, as shown in Figure 4, where thermal and molecular diffusion are equally important with convection. If l_T is the characteristic length of the heat transfer layer, the reaction zone has a thickness equal to l_T/Z. Expressions for l_T will be derived below.

The reaction zone and the heat transfer layer combine to form the combustion zone, Figure 4. Outside this zone, the problem is controlled by convective transport of energy and mass (and also by heat losses to the surroundings, if applicable). It is outside the combustion zone, where fluid dynamics and permeability heterogeneity are dominant. In the simplified example given previously, these would be regions I and III of Figure 1. Now, in all practical applications, the reaction zone has a sufficiently small width, so that it can be viewed as a front. Appropriate jump conditions can then be derived across it. In addition, it is likely that the heat transfer layer width is small compared to the fluid dynamical scale of the problem, l_S. If that is the case, we can define the small parameter $\delta = l_T/l_S$, and consider the combustion zone as a discontinuous front as shown in Figure 5. For such a description, additional jump conditions, now across the combustion front must be derived.

Before we proceed further, let us recall some basic notions related to front propagation. For simplicity, we will restrict our discussion to two-dimensional problems, although an extension to 3-D is straightforward. Consider a front propagating in the positive $\tilde{x}$ direction and described by

$$F(\hat{x}, \hat{y}, t) \equiv \hat{x} - f(\hat{y}, \hat{t}) = 0 \tag{7}$$

as shown in Figure 5. In our context, this equation separates a burned region ($F < 0$) from an unburned region ($F > 0$), where fresh solid fuel resides in the pore structure. Define the velocity of the surface by

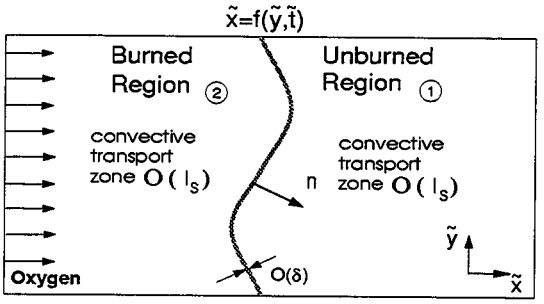

Figure 5: Combustion Front as a Discontinuity

$\boldsymbol{\nu}$. Then, from definition, the normal velocity with respect to a fixed frame of reference, ν_n, is

$$\nu_n \equiv \boldsymbol{\nu} \cdot \boldsymbol{n} = \frac{-F_t}{|\hat{\nabla} F|} = \frac{f_t}{(1+f_{\hat{y}}^2)^{1/2}} \tag{8}$$

where $f_t = \partial f/\partial t$ and $f_{\hat{y}} = \partial f/\partial \hat{y}$, and $\boldsymbol{n}$ is the unit vector normal to the front pointing in the direction of the unburned region

$$\boldsymbol{n} = \frac{\hat{\nabla} F}{|\hat{\nabla} F|}. \tag{9}$$

In the flame propagation literature, a useful quantity is the net normal velocity with respect to the moving front,

$$S_f \equiv \hat{\boldsymbol{v}}_{0^-} \cdot \boldsymbol{n} - \nu_n = \frac{\hat{v}_{\hat{x}} - \hat{v}_{\hat{y}} f_{\hat{y}} - f_t}{(1+f_{\hat{y}}^2)^{1/2}} \tag{10}$$

where $\hat{\boldsymbol{v}}_{0^-}$ is the average gas mixture velocity evaluated at $F = 0^-$. In the case of porous media, however, the above must be modified, due to the presence of the porous medium, to read as

$$S_{fp} \equiv \hat{\boldsymbol{v}}_{0^-} \cdot \boldsymbol{n} - \phi \nu_n = \frac{\hat{v}_{\hat{x}} - \hat{v}_{\hat{y}} f_{\hat{y}} - \phi f_t}{(1+f_{\hat{y}}^2)^{1/2}} \tag{11}$$

where ϕ is porosity. This and related quantities will be encountered below.

In the following, we will consider in sequence, first a reaction front, and then a combustion front. Using asymptotic expansions, the structure in both fronts will be analyzed and appropriate jump conditions across the fronts will be derived. To proceed, we need first to formulate the governing equations of the problem.

2.1 Governing Equations

Consider the combustion in a porous medium of a solid fuel, of known initial composition and concentration. In in-situ combustion, this fuel is in reality produced as a result of the LTO step, preceding the combustion front. Given that the two processes are coupled, the concentration and composition of the fuel is, in principle, not known a priori and must be determined as part of the solution of the overall problem. In the following, we will assume that the initial density of the fuel per unit total volume is known and given by ρ_f°.

At any time, the system consists of two phases, a solid phase including the solid matrix and the fuel, and a gas mixture of injected oxygen and reaction products. The matrix is non-reactive, stationary and its thermodynamic properties do not change during the process. The solid fuel reacts with injected oxygen, according to the following one-step heterogeneous reaction model

$$[\text{Fuel}] + \tilde{\gamma}\ [\text{Oxygen}] \longrightarrow \tilde{\gamma}_{gp}\ [\text{Gaseous Product}]$$

where we used pseudo-components for the fuel and the produced gases, and where $\tilde{\gamma}$ are stoichiometric coefficients. This simplification allows for a simple treatment of a complex problem. In formulating the conservation equations we will assume the following: locally, pore space and solid matrix are in thermal equilibrium, hence a one-temperature model is used for the energy balance; heat transfer by radiation, and energy source terms due to pressure increase, and work from surface and body forces are negligible; the

ideal gas law is the equation of state for the gas phase; thermodynamic and transport properties, such as conductivity, diffusivity, heat capacity of the solid, heat of reaction, etc. remain constant. We also define a conversion depth $\eta(\tilde{x},\tilde{y},\tilde{t}) = 1 - \rho_f/\rho_f^o$, such that $\eta = 0$ corresponds to the initial state and $\eta = 1$ to the case of complete fuel conversion.

Conservation equations are written for the following quantities: the total energy, the oxygen mass, the total gas mass and the fuel mass, in terms of the temperature $\tilde{T}(\tilde{x},\tilde{y},\tilde{t})$, the oxygen mass fraction $Y(\tilde{x},\tilde{y},\tilde{t})$, the average gas density $\rho_g(T,\tilde{p})$ and the fuel conversion depth. We also use Darcy's law for the flow of the gas phase, in terms of the pressure $\tilde{p}(\tilde{x},\tilde{y},\tilde{t})$. The dimensional form of these equations (superscript tilde) is shown below

energy

$$(1-\phi)c_s\rho_s\frac{\partial\tilde{T}}{\partial\tilde{t}} + c_g\rho_g\tilde{\boldsymbol{v}}\cdot\tilde{\nabla}\tilde{T} = \tilde{\nabla}\cdot(\lambda\tilde{\nabla}\tilde{T}) + \tilde{Q}\rho_f^o W - \dot{Q}_h \tag{12}$$

oxygen mass

$$\phi\frac{\partial(Y\rho_g)}{\partial\tilde{t}} + \tilde{\nabla}\cdot(Y\rho_g\tilde{\boldsymbol{v}}) = \tilde{\nabla}\cdot(D_M\rho_g\tilde{\nabla}Y) - \tilde{\mu}\rho_f^o W \tag{13}$$

total gas mass

$$\phi\frac{\partial\rho_g}{\partial\tilde{t}} + \tilde{\nabla}\cdot(\rho_g\tilde{\boldsymbol{v}}) = \tilde{\mu}_g\rho_f^o W \tag{14}$$

and depth of conversion

$$\frac{\partial\eta}{\partial\tilde{t}} = W \tag{15}$$

where, $\dot{Q}_h$ is a heat loss term and we introduced the rate of reaction W. Using the law of mass action we will take

$$W = k(\tilde{T})(Y\tilde{p})^m\psi(\eta) \tag{16}$$

where

$$k(\tilde{T}) = k_o e^{-E/R\tilde{T}} \tag{17}$$

E is the activation energy, k_o the pre-exponential factor, and m the exponent in the dependence on oxygen concentration and gas pressure. The dependence on η is through the dimensionless function ψ, the evaluation of which requires a more elaborate pore-level study [16]. Clearly, $\psi(1) = 0$.

In the above, c_i is the average specific heat capacity of species i (gas or solid) at constant pressure, ρ_i is the volumetric density of species i, and we assumed that the solid heat capacity is much larger than that of the gas. The average thermal conductivity, λ, is an effective value including the effects of gas and solid phases on conduction. Q represents the heat release of the fuel combustion reaction and is also assumed to be independent of temperature variations. Variable Y is the mass fraction of oxygen in the gas phase, D_M is an effective diffusion coefficient, while $\tilde{\mu}_g$ and $\tilde{\mu}$ are mass-weighted stoichiometric coefficients, $\tilde{\gamma}_i M_i/M_f$. The net gas production due to reaction is determined by the sign of $\tilde{\mu}_g = \tilde{\mu}_{gp} - \tilde{\mu}$ so that $\tilde{\mu}_g > 0$ or $\tilde{\mu}_g < 0$ corresponds to gas production or consumption, respectively. Finally, we have Darcy's law

$$\tilde{\nabla}\tilde{p} = -\frac{\eta_g}{k(\eta)}\tilde{\boldsymbol{v}} \tag{18}$$

where $k(\eta)$ is the permeability and η_g is the gas viscosity, and the equation of state, assuming ideal gases

$$\tilde{p}M_g = \rho_g R\tilde{T} \tag{19}$$

The expression for heat losses can take the simple form shown in (1) or the more elaborate expression

$$\dot{Q}_h = \frac{2\sqrt{\lambda_h c_h \rho_h}}{\sqrt{\pi}H}\int_0^{\tilde{t}} \frac{\partial \tilde{T}}{\partial \tau}\frac{\partial \tau}{\sqrt{\tilde{t}-\tau}} \tag{20}$$

reflecting heat conduction to a semi-infinite overburden and underburden (Yortsos and Gavalas [18]). Here subscript h refers to the surroundings and H is the reservoir thickness.

In the next section, we will proceed with a scaling and non-dimensionalization of the above equations.

2.2 Scaling and Non-dimensionalization

As described earlier, also shown in Figures 4 and 5, the problem includes three spatial scales, each associated with different dominant processes: the scale of a reactive-diffusive reaction zone, l_R, the scale of a convective-diffusive combustion zone, l_T, and the convective scale l_S. In the combustion zone, convection and conduction are of the same magnitude, namely the Peclet number, $Pe = v_* l_T c_s \rho_s / \lambda$ is of order 1, where the reference velocity v_* is to be determined. This defines l_T. If the front temperature of a planar combustion layer is $\tilde{T}_f$, also to be determined from the solution of the problem, then we have

$$
\begin{aligned}
l_R &\equiv \frac{l_T}{Z} \quad \text{where} \quad Z = \left[\frac{E\tilde{T}_o}{R\tilde{T}_f^2}\right], \\
l_T &\equiv \frac{\lambda}{v_* c_s \rho_s}, \\
l_S &\equiv \tilde{L}.
\end{aligned}
$$

The characteristic parameters to be chosen depend on what is the focus of the analysis. If it is the reaction zone, the characteristic time is based on the reaction kinetics

$$
t_R \equiv Z \left(k_o \tilde{p}_i^m e^{-E/R\tilde{T}_f}\right)^{-1}, \tag{21}
$$

and the characteristic length is the combustion zone length l_T. If the focus is on the combustion zone, then we rescale both the characteristic time and length by δ^{-1}, where $\delta = l_T/l_S \ll 1$. Then, $t_* = \delta^{-1} t_R$ and $x_* = \delta^{-1} l_T$. In either case, we have $v_* \equiv \frac{x_*}{t_*} = \frac{l_T}{t_R}$ where the reference velocity $v_* \equiv \frac{x_*}{t_*} = \frac{l_T}{t_R}$. This further implies the relation

$$
v_* = \sqrt{\frac{\lambda}{[(1-\phi) c_s \rho_s) t_R]}}. \tag{22}
$$

Scaling temperature with $\tilde{T}_o$ and density with the initial density ρ_{gi} and using the combustion zone formulation, we obtain the conservation equations in dimensionless form

$$\frac{\partial \theta}{\partial \hat{t}} + a\rho \boldsymbol{v} \cdot \hat{\nabla}\theta = \delta \hat{\Delta}\theta + \delta q \Phi - \dot{Q}_{hD} \tag{23}$$

$$\phi \frac{\partial (Y\rho)}{\partial \hat{t}} + \hat{\nabla} \cdot (Y\rho \boldsymbol{v}) = (\frac{\delta}{Le})(\hat{\nabla} \cdot \rho \hat{\nabla} Y) - \delta \mu \Phi \tag{24}$$

$$\phi \frac{\partial \rho}{\partial \hat{t}} + \hat{\nabla} \cdot (\rho \boldsymbol{v}) = \delta \mu_g \Phi \tag{25}$$

and

$$\frac{\partial \eta}{\partial \hat{t}} = \delta \Phi \tag{26}$$

where

$$\Phi \equiv \delta^{-2} Z (Yp)^m \psi(\eta) \exp\left[Z\theta_f^2 \left(\frac{1}{\theta_f} - \frac{1}{\theta} \right) \right] \tag{27}$$

In addition, we have

$$\hat{\nabla} p = -\kappa \boldsymbol{v} \tag{28}$$

and

$$\rho\theta = 1 + \Pi P. \tag{29}$$

In the above, we introduced the following variables and parameters

$$p = \frac{\tilde{p} - \tilde{p}_i}{\tilde{p}_{inj} - \tilde{p}_i}, \qquad \mu_i = \frac{\tilde{\mu}_i \rho_f^o}{\rho_{gi}}, \qquad \dot{Q}_{hD} = \frac{\dot{Q}_h t_R}{T_o \delta c_s \rho_s}, \qquad a = \frac{c_g \rho_{gi}}{c_s \rho_s}, \qquad \Phi = \delta^{-1} W t_*,$$

$$q = \frac{Q\rho_f^o}{c_s \rho_s \tilde{T}_o}, \qquad Le = \frac{\lambda}{D_M (1-\phi) c_s \rho_s}, \qquad \kappa = \frac{\eta_g x_* v_*}{k(\tilde{p}_{inj} - \tilde{p}_i)}, \Pi = \frac{\tilde{p}_{inj} - \tilde{p}_i}{\tilde{p}_i},$$

where $\tilde{p}_i$ and $\tilde{p}_{inj}$ are the initial and the injection gas pressure in the system. Note that the spatial coordinates are nondimensionalized based on the system length, l_S, which in the limit $\delta \ll 1$ allows to approximate the combustion zone as a thin layer. To focus on the combustion zone, we simply change the scaling, which is equivalent to taking $\delta = 1$ in the above equations.

The boundary conditions depend on the extent of the combustion process. If we assume that the fuel is fully consumed, we will take for $\hat{t} \geq 0$:

$$Y = 1, \qquad \theta = \theta_f \qquad \eta = 1 \qquad ; \qquad \hat{x} \to -\infty \tag{30}$$

$$Y = Y_b, \qquad \theta = 1, \qquad \eta = 0 \qquad ; \qquad \hat{x} \to \infty \tag{31}$$

where θ_f and Y_b are to be determined. This is the fuel-deficient case. Otherwise, we have

$$Y = 1, \qquad \theta = \theta_f \qquad \eta = \eta_f \qquad ; \qquad \hat{x} \to -\infty \tag{32}$$

$$Y = 0, \qquad \theta = 1, \qquad \eta = 0 \qquad ; \qquad \hat{x} \to \infty \tag{33}$$

where θ_f and η_f are to be determined. This is the oxidant-deficient case. In the following, we will consider only the fuel-deficient case.

2.3 Moving Coordinates

The final step in the formulation of the problem is to convert to moving coordinates, moving with the combustion front, which in the fuel-deficient case can be defined as the position at which $\eta = 1/2$. If we denote $x = \hat{x} - f(\hat{y}, \hat{t})$, $y = \hat{y}$ and $t = \hat{t}$, then the non-dimensional equations take the form:

$$\frac{\partial \theta}{\partial t} + \{a\rho s - f_t\} \frac{\partial \theta}{\partial x} + a\rho v_y \frac{\partial \theta}{\partial y} = \delta \Delta \theta + \delta q \Phi - \dot{Q}_{hD} \tag{34}$$

$$\phi\frac{\partial(Y\rho)}{\partial t}+\frac{\partial[Y\rho(s-\phi f_t)]}{\partial x}+\frac{\partial}{\partial y}(Y\rho v_y)=\left(\frac{\delta\rho}{Le}\right)\Delta Y-\delta\mu\Phi \tag{35}$$

$$\phi\frac{\partial\rho}{\partial t}+\frac{\partial[\rho(s-\phi f_t)]}{\partial x}+\frac{\partial}{\partial y}(\rho v_y)=\delta\mu_g\Phi \tag{36}$$

$$\frac{\partial\eta}{\partial t}-f_t\frac{\partial\eta}{\partial x}=\delta\Phi$$

$$\kappa v_x=-\frac{\partial p}{\partial x} \tag{37}$$

$$\kappa v_y=-\left[\frac{\partial p}{\partial y}+f_y\frac{\partial p}{\partial x}\right] \tag{38}$$

$$\rho\theta=1+\Pi p \tag{39}$$

Here,

$$s\equiv v_x-v_y f_y, \tag{40}$$

is the longitudinal velocity of the gas mixture in the moving frame and we defined the Laplace operator in moving coordinates

$$\Delta\equiv(1+f_y^2)\frac{\partial^2}{\partial x^2}+\frac{\partial^2}{\partial y^2}-\frac{\partial^2 f}{\partial y^2}\frac{\partial}{\partial x}-2\frac{\partial f}{\partial y}\frac{\partial^2}{\partial x\partial y}, \tag{41}$$

For simplicity in the presentation, the density term in the diffusion of oxygen was approximated as constant. However, this approximation is not made in the subsequent analysis. Having obtained the desired formulation, we proceed next with the analysis of the structure of the reaction zone and then with that of the combustion zone.

3 The Reaction Zone

Under the condition $Z \gg 1$, the reaction zone thickness, l_T/Z, is much smaller than l_T. To analyze the structure of the zone, we stretch the longitudinal moving coordinate, $X = Zx$, and expand the dependent variables in asymptotic series in Z^{-1}. Following [8] it can be shown that, to leading order, temperature, concentration, pressure and density are independent of X. Thus, we take

$$\theta \sim \theta^o(y,t) + Z^{-1}\theta^1(X,y,t) + \ldots,$$

$$Y \sim Y^o(y,t) + Z^{-1}Y^1(X,y,t) + \ldots,$$

$$p \sim p^o(y,t) + Z^{-1}p^1(X,y,t) + \ldots,$$

$$\rho \sim \rho^o(y,t) + Z^{-1}\rho^1(X,y,t) + \ldots,$$

$$\eta \sim \eta^o(X,y,t) + \ldots,$$

$$s \sim s^o(X,y,t) + \ldots,$$

$$v_y \sim v_y^o(y,t) + \ldots,$$

$$f \sim f^o(y,t) + \ldots.$$

The respective leading-order terms are obtained after substitution in the governing equations. Combining the energy equation with the fuel balance, shows that the leading-order terms are $O(Z^{-1})$, in which case only conduction in the X direction and reaction participate, namely

$$\delta\left[1 + f_y^{o2}\right]\frac{\partial^2\theta^1}{\partial X^2} = q f_t^o \frac{\partial \eta^o}{\partial X} \tag{42}$$

(note that the heat loss term vanishes to leading order). For the oxygen mass balance, a similar analysis shows that the leading-order terms are convection, diffusion and reaction, hence

$$Le\rho^o Y^o(y,t)\frac{\partial s^o}{\partial X} - \delta\rho^o\left[1 + f_y^{o2}\right]\frac{\partial^2 Y^1}{\partial X^2} = \mu Le f_t^o \frac{\partial \eta^o}{\partial X}, \tag{43}$$

where we have taken into account that ρ^o is constant, while the total gas mass balance reads

$$\rho^o \frac{\partial s^o}{\partial X} = -\mu_g f_t^o \frac{\partial \eta^o}{\partial X}. \tag{44}$$

The equation for the fuel mass is expressed to leading-order as

$$\delta f_t^o \frac{\partial \eta^o}{\partial X} = -\frac{[Y^o(y,t)p^o(y,t)]^m}{\psi(\eta^o)} e^{\theta^1} \tag{45}$$

where we used a power series expansion for the exponential term. Finally, to leading-order, pressure is constant within the reaction zone.

Integrating equations (42- 44) across the reaction zone determines the jumps in heat, oxygen mass and gas mass fluxes across the front in terms of the jump in depth of fuel conversion,

$$\delta \left[1 + f_y^{o2}\right] \left.\frac{\partial \theta^1}{\partial X}\right|_{-\infty}^{\infty} = q f_t^o \eta^o \,|_{-\infty}^{\infty} \tag{46}$$

$$\delta \left[1 + f_y^{o2}\right] \left.\frac{\partial Y^1}{\partial X}\right|_{-\infty}^{\infty} = -\left[\mu + Y^o(y,t)\mu_g\right] Le f_t^o \, \eta^o|_{-\infty}^{\infty} \tag{47}$$

$$\rho^o s^o \,|_{-\infty}^{\infty} = -\mu_g f_t^o \, \eta^o|_{-\infty}^{\infty}. \tag{48}$$

The depth of conversion equation (45) can also be integrated across the reaction zone. For this, we first integrate equation (42) using the boundary conditions $\partial\theta^1/\partial X = 0$, $\eta^o = 1$ as $X \to -\infty$, to give

$$\delta \left[1 + f_y^{o2}\right] \frac{\partial \theta^1}{\partial X} = -q f_t^o (1 - \eta^o) \tag{49}$$

Then, multiplying equation (49) by (45) yields

$$q\,(f_t^o)^2 \left(\frac{1-\eta^o}{\psi(\eta^o)}\right) \frac{\partial \eta^o}{\partial X} = -\left[1 + f_y^{o2}\right] [Y^o(y,t)p^o(y,t)]^m \, e^{\theta^1} \frac{\partial \theta^1}{\partial X} \tag{50}$$

This equation can be now integrated across the reaction zone, to give the following result for the square of the normal front velocity

$$\frac{\left(f_t^o\right)^2}{1+f_y^{o2}} = \frac{[Y^o(y,t)p^o(y,t)]^m}{q\int_0^1 \frac{(1-\eta^o)}{\psi(\eta^o)}d\eta^o}. \tag{51}$$

We note that the expression for the normal front velocity is primarily related to the unknown mass fraction of the oxidant at the completion of the reaction and the pressure at the front.

Conditions (46-48) also express the jump of the corresponding quanities across the reaction zone. Namely, if we define the jump in a quantity of the combustion zone π across the reaction front as $[\pi]_-^+ = \pi\,(x=0^+) - \pi\,(x=0^-)$, we obtain for the deficient-fuel case (where $\eta^o|_{-\infty}^{\infty} = 0-1=-1$)

$$[Y]_-^+ = [\theta]_-^+ = [p]_-^+ = 0, \qquad [\eta]_-^+ = -1, \tag{52}$$

and

$$\begin{aligned} \delta\left[1+f_y^{o2}\right]\left[\frac{\partial\theta}{\partial x}\right]_-^+ &= -qf_t \\ \delta\left[1+f_y^{o2}\right]\left[\frac{\partial Y}{\partial x}\right]_-^+ &= [\mu + Y^o(y,t)\mu_g]\,Lef_t \\ [\rho(s-\phi f_t)]_-^+ &= \mu_g f_t, \end{aligned} \tag{53}$$

In the above we have assumed full consumption of the fuel at *any* point of the front.

4 The Combustion Zone

Consider, next, the combustion zone structure. Outside the reaction zone, the chemical reaction rates are insignificant. To analyze this problem, we must consider the conservation equations to either side of the reaction front, across which the jump conditions derived previously apply. For this, we need to consider an

expansion valid inside the combustion zone, in which conduction and diffusion, but not chemical reaction, are taken into account.

In the context of the overall problem (Figure 5), the combustion zone has a dimensionless extent of order δ, hence we must introduce the stretched coordinate $\xi = x/\delta$ and seek inner expansions of the following form

$$\begin{aligned}
\theta &\sim \theta_o + \delta\theta_1 + \ldots, \\
Y &\sim Y_o + \delta Y_1 + \ldots, \\
p &\sim p_o + \delta p_1 + \ldots, \\
\rho &\sim \rho_o + \delta\rho_1 + \ldots, \\
\eta &\sim \eta_o + \delta\eta_1 + \ldots, \\
s &\sim s_o + \delta s_1 + \ldots, \\
v_y &\sim v_{yo} + \delta v_{y1} + \ldots, \\
f &\sim f_o + \delta f_1 + \ldots,
\end{aligned}$$

These expansions are then introduced in the equations in moving coordinates. Under the condition $\frac{ht_R}{(1-\phi)c_g\rho_g} \ll 1$, the heat loss term does not contribute to leading order, thus the energy balance reads

$$A_o \frac{\partial \theta_o}{\partial \xi} - \left[1 + f_{oy}^2\right] \frac{\partial^2 \theta_o}{\partial \xi^2} = 0 \tag{54}$$

where

$$A_o(\xi, y, t) = a\rho_o s_o - f_{o_t} \tag{55}$$

and

$$s_o = v_{xo} - v_{yo} \frac{\partial f_o}{\partial y} \tag{56}$$

Oxygen, total gas and fuel mass balances become, respectively,

$$\rho_o B_o \frac{\partial Y_o}{\partial \xi} - \frac{1}{Le}\left[1 + f_{oy}^2\right]\frac{\partial}{\partial \xi}\left[\rho_o \frac{\partial Y_o}{\partial \xi}\right] = 0 \tag{57}$$

$$\frac{\partial}{\partial \xi}\left[\rho_o B_o\right] = 0 \tag{58}$$

$$\frac{\partial \eta_o}{\partial \xi} = 0 \tag{59}$$

where

$$B_o(\xi, y, t) = s_o - \phi f_{o_t}. \tag{60}$$

Darcy's law gives

$$\frac{\partial p_o}{\partial \xi} = 0 \tag{61}$$

and the ideal gas law reads

$$\rho_o \theta_o = \text{const.} \tag{62}$$

Parameter a, representing the ratio of gas to solid heat capacities is small, thus, we expect $A_o < 0$. Also, for a propagating front along the positive x direction, we must have $s_o > \phi f_{o_t}$, hence $B_o > 0$. Experimental data obtained in combustion tube experiments (e.g. see Martin et al. [19], or Mamora and Brigham [20]), confirm these assumptions. We can then proceed to integrate the above equations.

Because $A_o < 0$, the only possible solution for θ_o in the region $\xi < 0$ is a constant independent of ξ (otherwise, θ_o will become unbounded as $\xi \to -\infty$). To find the solution for $\xi > 0$, we integrate (54) and make use of the jump condition at the reaction front

$$\left[1 + f_{oy}^2\right]\left[\frac{\partial \theta_o}{\partial \xi}\right]_-^+ = -q f_{o_t} \tag{63}$$

to obtain the result

$$\theta_o = \begin{cases} \theta_f(y,t) & : \ \xi < 0 \\ 1 - \dfrac{q f_{o_t}}{A_o} e^{\left[\dfrac{A_o}{\left[1+f_{o_y}^2\right]}\xi\right]} & : \ 0 < \xi \end{cases}$$

showing that the temperature decays exponentially fast downstream of the combustion front.

Working similarly, equation (57) shows that because $B_o > 0$, the solution for Y in $\xi > 0$ must be a constant independent of ξ. Equation (58) also shows that $\rho_o B_o$ is a constant. Then, by integrating (57) in the region $\xi < 0$, where ρ_o is constant, and making use of the jump condition across the reaction front,

$$\left[1+f_{o_y}^2\right]\left[\frac{\partial Y_o}{\partial \xi}\right]_-^+ = (\mu + Y_b(y,t)\mu_g)\, Le f_{o_t} \tag{64}$$

we obtain the final result

$$Y_o = \begin{cases} 1 - \left[\dfrac{(\mu + Y_b\mu_g) f_{o_t}}{B_o}\right] e^{\left[\dfrac{LeB_o}{\left[1+f_{o_y}^2\right]}\xi\right]} & : \ \xi < 0 \\ Y_b(y,t) & : \ 0 < \xi \end{cases}$$

This equation gives the profile of the mass fraction upstream of the reaction front. Fianlly, equation (59) gives the expected result

$$\eta_o = \begin{cases} 1 & : \ \xi < 0 \\ 0 & : \ 0 < \xi \end{cases}$$

assuming, again, complete fuel combustion. Figure 6 show schematic profiles of temperature, mass fraction and conversion across the combustion zone.

Note that A_o in the temperature equation involves the mass flux $\rho_o s_o$ downstream of the reaction front (although its contribution to A_o may be very small due to $a \ll 1$), while B_o in the mass fraction expression

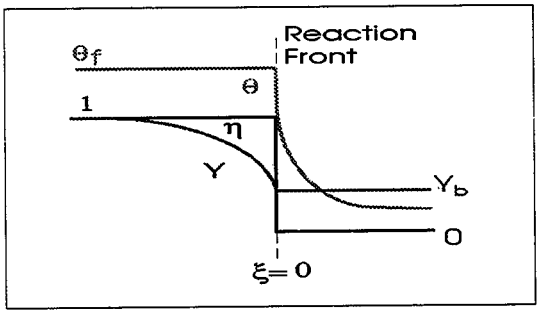

Figure 6: Schematic Profiles of Temperature, Oxygen Mass Fraction and Conversion in the Combustion Zone.

involves the mass flux upstream of the reaction front. The two fluxes are related to each other through the jump condition

$$[\rho s]_-^+ = \mu_g f_t \tag{65}$$

derived in equation (54). The above equations represent the leading order "inner" expansion to the large scale problem, for which the combustion front appears as a discontinuity. In the section to follow we will consider the "outer" problem, on either side of the front (see Figure 5) by keeping only the convective transport term in the equations. To match the outer expansions we use the jump conditions derived from the inner problem, namely the problem in the combustion zone. These were derived previously to leading-order, and are summarized below.

$$\begin{aligned} [\theta_o] &= 1 - \theta_f(y,t) \\ [Y_o] &= Y_b(y,t) - 1 \\ \left[\rho_o(s_o - \phi f_{o_t})\right] &= \mu_g f_{o_t} \\ [\eta_o] &= -1 \\ [p_o] &= 0 \end{aligned} \tag{66}$$

$$\left[\frac{\partial \theta_o}{\partial \xi}\right] = \left[\frac{\partial Y_o}{\partial \xi}\right] = \left[\frac{\partial p_o}{\partial \xi}\right] = 0$$

These equations must be considered along with equation (51) for the normal front velocity, where $Y^o(y,t) = Y_b$.

5 The Convective Transport Region

The scale of the outer problem is the scale of the originally derived equations. Here, conduction, diffusion and reaction (but not heat losses) are negligible, and we seek expansions of the form

$$\theta \sim \Theta_o + \delta\Theta_1 + \ldots,$$

$$Y \sim \Upsilon_o + \delta\Upsilon_1 + \ldots,$$

$$p \sim P_o + \delta P_1 + \ldots,$$

$$\rho \sim R_o + \delta R_1 + \ldots,$$

$$s \sim S_o + \delta S_1 + \ldots,$$

$$v_y \sim V_{yo} + \delta V_{y1} + \ldots.$$

Direct substitution in the original equations shows that the leading term of the expansions satisfy the following

$$\frac{\partial \Theta_o}{\partial t} + (aR_oS_o - f_{o_t})\frac{\partial \Theta_o}{\partial x} + aR_oV_{yo}\frac{\partial \Theta_o}{\partial y} = -\dot{Q}_{hD} \tag{67}$$

$$\phi\frac{\partial(\Upsilon_oR_o)}{\partial t} + \frac{\partial[\Upsilon_oR_o(S_o - \phi f_{o_t})]}{\partial x} + \frac{\partial(\Upsilon_oR_oV_{yo})}{\partial y} = 0, \tag{68}$$

$$\phi\frac{\partial R_o}{\partial t} + \frac{\partial(R_o(S_o - \phi f_{o_t})}{\partial x} + \frac{\partial(R_oV_{yo})}{\partial y} = 0, \tag{69}$$

$$\kappa V_{xo} = -\frac{\partial P_o}{\partial x}, \tag{70}$$

$$\kappa V_{yo} = -\left[\frac{\partial P_o}{\partial y} + f_{oy}\frac{\partial P_o}{\partial x}\right], \tag{71}$$

$$R_o\Theta_o = 1 + \Pi P_o, \tag{72}$$

$$S_o = V_{xo} - V_{yo}\left(\frac{\partial f_o}{\partial y}\right). \tag{73}$$

The fuel mass balance shows that the convective derivative of η_o in the moving coordinate system vanishes, implying that the depth of fuel conversion is constant in both regions, as expected,

$$\eta = \begin{cases} 1 & : \ x < 0 \\ 0 & : \ 0 < x. \end{cases}$$

The solution of the outer problem must be considered in the two regions on either side of the combustion front, across which the jump conditions previously derived apply. The solution can be attempted using the method of characteristics, or the method of streamlines depending on the complexity of the geometry and heterogeneity in permeability. In the general case, the problem must be solved numerically.

In the following section, we illustrate the application of the previous results by considering the particular example of a planar front.

6 Case of a Planar Front

For the case of a planar front, we have $A_o = am^+_{oD} - V_D$, where m^+_{oD} is the dimensionless mass flux downstream of the front and V_D is the dimensionless front velocity. Using the expression for the temperature profile inside the combustion zone, in conjunction with the continuity of temperature at $\xi = 0$, $[\theta_o]^+_- = 0$, gives an expression for the dimensionless temperature at the front, which reads as follows

$$\theta_f = 1 - \frac{q_D V}{am^+_{oD} - V_D}. \tag{74}$$

Note that $m_{oD}^{+} = m_{oD}^{-} + \mu_g V_D$ where m_{oD}^{-} is the incoming mass flux. Equation (74) is a more rigorous dimensionless expression for the temperature jump across the front, compared to equation (4). Note that if $am_{oD}^{+} \ll 1$, then θ_f is the adiabatic temperature rise

$$\theta_f = 1 + q \tag{75}$$

However, this is not generally the case. In the planar case, the dimensionless velocity is given from

$$V_D^2 = \frac{(Y_b p^o)^m}{q \int_0^1 \frac{(1-\eta^o)}{\psi(\eta^o)} d\eta^o}. \tag{76}$$

the calculation of which requires an expression for Y_b. This is obtained from the expression for the oxygen mass fraction within the combustion zone, along with the requirement of continuity at $\xi = 0$, hence

$$Y_b = \frac{m_{oD}^{-} - (\phi + \mu) V_D \rho_o}{m_{oD}^{-} + (\mu_g - \phi) V_D \rho_o} \tag{77}$$

Note that for $Y_b > 0$, the condition $m_{oD}^{-} > (\phi + \mu) V_D \rho_o$ must apply, namely the total gas mass flux should be sufficiently large.

Expressed in dimensional form, equations (74), (76), (77) and equation (22) form a system of four algebraic equations in the four unknowns, T_f, V_D, Y_b and v_*. The problem was solved numerically for the parameter values shown in Table 1. Before we proceed, let us note that for a burning temperature of 600°F, we have l_T =1.25 inch (3.18 cm) for the combustion zone thickness, and l_R =0.19 inch (0.48 cm) for the thickness of the reaction zone. The very small thickness of these zones should be carefully considered in the implementation of direct numerical simulation of in-situ combustion, particularly at the field scale. Results for the dimensionless velocity of the front V_D and Y_b are shown in Figures 7 and 8 as a function of the normalized injection velocity $\frac{\rho_{gi}}{\rho_f^o} v$. As expected, both variables increase with the injection velocity.

Table 1: **Typical Values of Porous Medium and Fluid Parameters for Combustion**

Parameter	Value
$\tilde{Q}$	20,000 Btu/lbmole fuel
E	25,000 Btu/lbmole
R	1.987 Btu/lbmole-R
k_o	100 $s^{-1}atm^{-1}$
$\tilde{T}_o$	140 F
m	1
$\tilde{v}$	50 ft/D
$\tilde{P}_i$	5 atm.
λ	12 Btu/ft-D-F
ϕ	0.3
ρ_{gi}	0.0765 lbm/ft^3
$c_g\rho_{gi}$	0.0184 Btu/ft^3-F
ρ_f^o	58.3 lbm/ft^3
$c_s\rho_s$	35 Btu/ft^3-F
M_f	235 lbm/lbmole
$\psi(\eta)$	1-η
μ	2,300
μ_g	764

Source: References [2] and [12]

7 Concluding Remarks

In this paper, we proposed a method for modeling the propagation of combustion fronts in porous media, by treating the reaction region as a place of discontinuities in the appropriate variables, which include, for example, fluxes of heat and mass. It was shown that reaction and combustion fronts have a spatially narrow width, estimated to be of the order of cm, within which heat release rates, temperatures and species concentrations vary significantly. The narrow width calls for an approach in which these fronts are treated as surfaces of discontinuity.

Using a rigorous perturbation approach, similar to that used in the propagation of flames [3] and smoldering

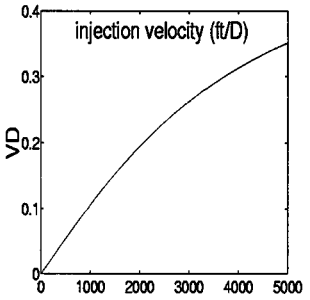

Figure 7: Injection Velocity versus the Front Velocity

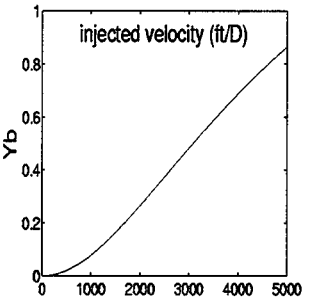

Figure 8: Injection Velocity versus the Unburned Oxygen Concentration

combustion [7], we derived appropriate jump conditions that relate the change in these variables across the front to leading order. The conditions account for the kinetics of the reaction between the oxidant and the fuel, the changes in the morphology of the pore space and the heat and mass transfer in the reaction zone. Then, the modeling of the problem reduces to the modeling of the dynamics of a combustion front, on the regions of either side of which convective transport of momentum (fluids), heat and mass, but not chemical reactions, must be considered. Properties of the two regions are coupled using the derived jump conditions. This methodology allows to explicitly incorporate permeability heterogeneity effects in the process description, without the undue complexity of the coupled chemical reactions.

For the case of 1-D planar fronts, we derived explicit expressions, which allow to obtain the burning temperature, the front velocity and the amount of oxygen left unreacted, in terms of the process variables, such as injection rates and pressure. For the case of fronts in two and three dimensions, particularly in heterogeneous porous media, a numerical method must in general be implemented. The analysis described must be extended to include higher-order terms in the small parameter δ. In progress is a stability analysis of the front, which also includes higher-order terms. Also neglected in the examples were heat losses In any case, however, the proposed treatment of the front as a discontinuity calls for a different approach in the simulation and upscaling, when coarse grids, such as those at the field scale, must be used. Because of the hyperbolic nature of the equations in the outer regions, methods based on characteristics and, more generally, on front tracking would appear to be appropriate. However, a direct implementation of existing methods, for instance of streamline simulation, is not feasible, because fluid and temperature streamlines are generally not the same, due to the difference in the volumetric heat capacities of gas and solid. In addition, the front temperature and reacted mass fraction are to be obtained from the solution of the overall problem. Further research is needed in this direction.

8 Acknowledgements

This research was partly supported by DOE Contract DE-AC26-99BC15211, the contribution of which is gratefully acknowledged.

References

[1] Prats, M: "Thermal Recovery," *SPE Monograph Series* SPE of AIME (1982).

[2] Boberg, T.C: "Thermal Methods of Oil Recovery" *An Exxon Monograph Series* (1988).

[3] Matalon, M. and Matkowsky B.J.: "Flames as Gasdynamic Discontinuities," *J. Fluid Mech.* (1982) **124** 239-259.

[4] Pelcé, P.: "Dynamics of Curved Fronts," *J. Academic Press* (1988).

[5] Aldushin, A.P., Matkowsky, B.J.: "Instabilities, Fingering and the Saffman-Taylor Problem in Filtration Combustion," *Combust. Sci. and Tech.* (1998) **133**.

[6] Li, X. and Yortsos, Y.C.: "Bubble Growth and Stability in an Effective Porous Medium," *Phys. Fluids* (1994) **6** (5) 1663-77.

[7] Schult, D.A., Matkowsky, B.J., Volpert, V.A., and Fernandez-Pello, A.C.: "Forced Forward Smolder Combustion," *Combust. and Flame* (1996) **104** 1-26.

[8] Schult, D.A., Bayliss, A. and Matkowsky, B.J.: "Traveling Waves in Natural Counterflow Filtration Combustion and Their Stability," *SIAM J. Appl. Math.* (1998) **58** No.3 806-852.

[9] Gottfried, B.S.: "A Mathematical Model of Thermal Oil Recovery in Linear Systems," *SPEJ* (1965) 196-210

[10] Beckers, H.L. and Harmsen, G.J.: "The Effect of Water Injection on Sustained Combustion in a Porous Medium" *SPEJ* (1970) 231-49.

[11] Burger, J.G. and Sahuquet, B.C.: "Chemical Aspects of *In Situ* Combustion — Heat of Combustion and Kinetics," *SPEJ* (1972) 54-66.

[12] Ağca, C. and Yortsos, Y.C.:"Steady-State Analysis of *In Situ* Combustion," Paper SPE 13624, presented at California Regional Meeting of SPE, Bakersfield, 447-362 (March 27-29 1985).

[13] Armento M.E. and Miller, C.A.: "Stability of Moving Combustion Fronts in Porous Media," *SPEJ* (1977) 423-430.

[14] Britten, J.A., Krantz, W.B.: "Linear Stability of Planar Reverse Combustion in Porous Media," *Combust. and Flame.* (1985) **60** 125-240.

[15] Britten, J.A., Krantz, W.B.: "Asymptotic Structure of Planar Nonadiabatic Reverse Combustion Fronts in Porous Media," *Combust. and Flame.* (1986) **65** 151-161.

[16] Lu, C. and Yortsos, Y.C.: To be submitted.

[17] Zik, O., Moses E.: "Fingering Instability in Combustion: An Extended View," *Physical Rev. E* (1999) **60** 1518-1531.

[18] Yortsos, Y.C. and Gavalas, G.R.: "Heat Transfer Ahead of Moving Condensation Fronts in Thermal Oil Recovery Processes," *Int. J. Heat Mass Transfer*(1982) **305** No.3 305-316.

[19] Martin, W.L., Alexander, J.D. and Dew, J.N.: "Process Variabes of In Situ Combustion," *Petroleum Trans.* AIME (1958) **213** 28-35.

[20] Mamora, D.D., Brigham, W.E.: "Implications of Low Temperature oxidation in Kinetic and Combustion Tube Experiments," UNITAR 6th. Symposium on Heavy Oil and Tar Sands (1995).